THE CORROSION RESISTANCE OF AN Al–Li ALLOY IN 3.5 wt.–% NaCl①

Liu, Haiping② Yan, Yumin③ Yuan, Guansen④

General Research Institute for Non-ferrous Metals, Beijing,100088, China

ABSTRACT

The influences of heat treatment and pH value on corrosion potential and cyclic polarization curve of an Al–Li alloy in 3.5 wt.–% NaCl were investigated. Microstructures of the alloy were combined to analyze and explain the development of cyclic polarization curves and the variation of corrosion potential within 24 h. The results revealed that the preferential dissolution of the precipitates in the alloy increased the susceptibility of the alloy to localized corrosion. Prolonging artificial ageing treatment caused heavy precipitation of T1 phase in matrix and both precipitation of phases containing copper and widening of PFZ along the grain boundary, and thus worsened the corrosion resistance. In strong acidic or strong alkaline solution the alloy demonstrates poor corrosion resistance.

Key words: Al–Li alloy, Corrosion, polarization, pitting, passivation.

1 INTRODUCTION

Al–Li alloy possesses a profound application in aerospace industry for their low density and high intensity, their corrosion behavior has become of great interest. The investigation displayed that both chemical compositiom and heat treatment parameters affect the corrosion resistance by modifying microstructures of the alloy [1-3]. Overaging was commonly thought detrimental to the corrosion resistance of binary alloys by increasing activity of grain boundary[4]. To some multi-element alloys the occurrence of δ' (Al_3Li) phase and T1 (Al_2CuLi) phase in artificial duration were considered to be responsible for SCC and pitting attacks[5-7]. However, some alternative conclusions were reported[1,8]. Besides material factors, environment conditions also influence the corrosion behavior[9]. Craig[10] demonstrated that 8090 alloy possesses a high passivation current density in alkaline solution. Motan[2] and Ohsaki[11] found that this alloy and an AlCuLiMg alloy are susceptible to pitting attack in solution containing Cl^- ions and the corresponding cyclic polarization curves consisted of several sections, indicating the occurence of a complicated electrochemical process. In a word, although much information has been collected , the action of each precipitate in the corrosion process and the electrochemical reactions at the electrode / solution interface or within localized corrosion areas need studies further.

①Mauscript received August 25, 1991

②Dr.; ③Associate Engineer; ④Professor

The purpose of this paper is to investigate the influences of heat treatment and solution acidity on cyclic polarization curve and corrosion potential of an Al–Li alloy, and to illustrate the relationship between the corrosion behavior and its microstructure.

2 EXPERIMENT

A PM–RSP Al 4.50 Cu 1.77 Li 0.52 Mg 0.20 Zr alloy rod with a 17 mm in diameter was hot rolled to a 1.0–1.3 mm thick sheet. After being divided into five parts, each was prepared according to one of the heat treatment states listed in Table 1. Then, they were cut into 1×1 cm^2 size and polished with SiC papers to 800 grits. Electrochemical measurements were taken in 3.5 wt.–% NaCl solution at 293 ± 2 Kwith an EG & G model 351 system and a model 273 potentiostat. A platimium sheet and a saturated calomel electrode were employed as an auxiliary electrode and a reference electrode respectively. The pH of the solution was adjusted with HCl and NaOH solutions. Corrosion potential and its variation with immersion time were measured in aerated solution, whereas polarization resistance and cyclic polarization curve were measured in de-aerated solution with high purity nitrogen 30 min prior to and throughout the tests. Polarization resistance measurement was conducted in $E_{corr} \pm 20$ mV range with 0.1 mV / s. Cyclic polarization was initiated at a potential 300–600 mV below corrosion potential with 0.166 mV / s towards electropositive direction. When the anodic current density reached about 20 mA / cm^2, the scan was reversed. A JSM–35C SEM was used to observe the specimen surface after anodicly polarized to 20 mA / cm^2. The TEM thin foils were obtained with a dual jet apparatus by using nitric acid and methanol mixture (2:1 *V* / *V*) at 243 K and a potential difference of 10–12 V. A JCEM 2000 FX TEM with EDAX was employed to observe microstructure of the alloy.

3 RESULTS AND DISCUSSION

3.1 *Effect of Heat Treatment on Microstructure*

Fig.1 shows TEM micrographs of the alloy under various heat treatment states. No recognizable precipitate and PFZ can be seen in hot rolled and natural aged specimens. However, artificial aging induced the precipitation of spherical δ' phase mainly in unedraged alloy and needle T1 phase mainly in peakaged and overaged specimens. Also prolonging artificial aging caused heterogeneous precipitate containing high copper and PFZ along the grain boundary. Table 1 indicates that the intensity of the alloy can be significantly increased by solution treatment plusing artificial aging. Compating with TEM observation, one can assume that T1 phase is more effective than δ' phase in intensifying the alloy. The slight decrease of microhardness of overaged alloy probably results from the precipitation of equilibrium phases along the grain boundary and the destruction of lattice between T1 phase and matrix.

3.2 *Effects of Heat Treatment and* pH *on Corrosion Potential*

Table 1 illustrates that the corrosion potential is elevated about 100 mV after solution treatment. Supersaturated copper in aluminium lattice is probly responsible for this change. Because δ' phase and T1 phase are anodic to matrix[12,13], their distribution in matrix can decrease the combined apparent

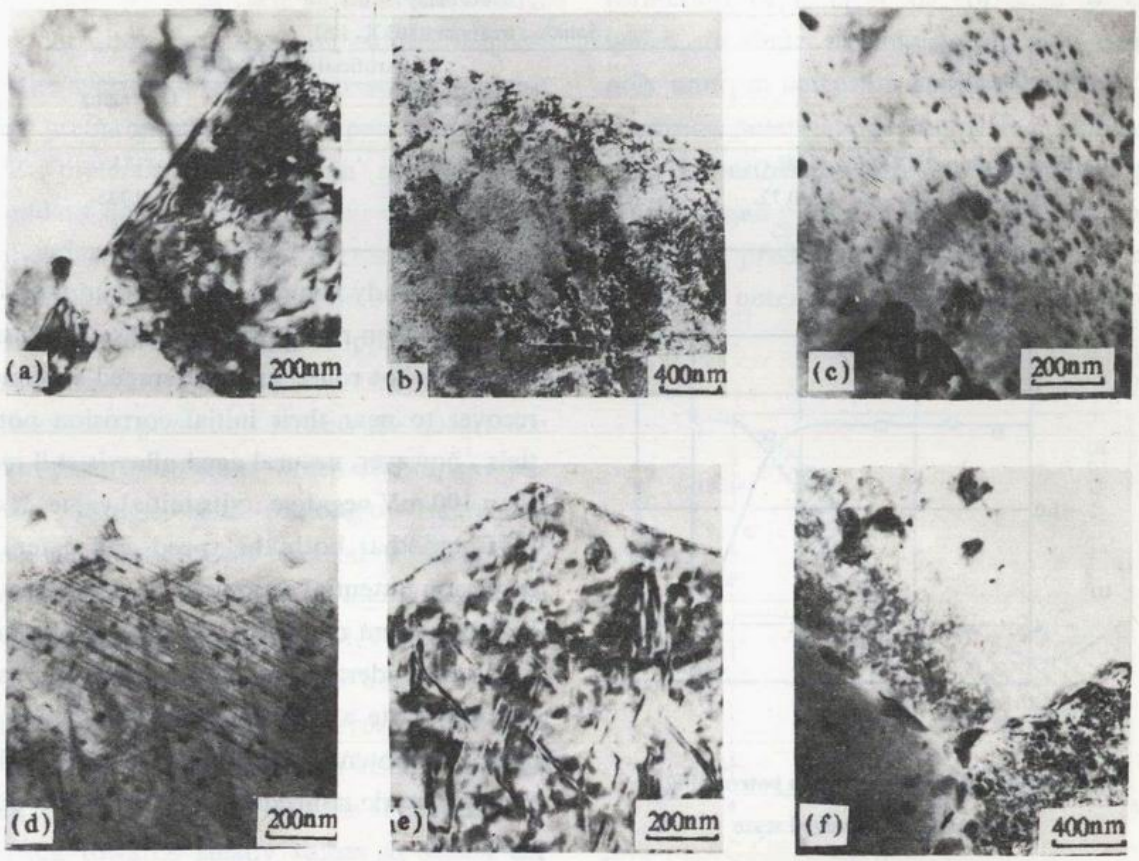

Fig.1 TEM micrographs of the alloy under the heat treatment conditions in Table 1

a——hot rolled and natural aged; b, c——underaged; d–f——peakaged and overaged

corrosion potential, and the alloy containing more precipitates should show lower corrosion potential. The evidence in Table 1 affirms this inference. Additionally although with a wider PFZ and a greater amount of precipitate along the grain boundary, the overaged alloy has a corrosion potential just 10 mV negative to that on peakaged alloy. This suggests that the corrosion potential is mainly determined by the behavior of the matrix. It had been reported that a more negative corrosion potential appeared on δ' phase rather than on T1 phase[12,13]. Accordingly, more negative corrosion potential should appear on underaged specimen instead of on peakaged or overaged alloy. The inversion, in fact, can be explained from their polarization resistances in Table 1. According to Evans′ polarization diagram[14], it is possible for underaged alloys with more anodic phase but with higher polarization resistances to show a higher corrosion potential. As no recognizable precipitates in hot rolled alloy, its low corrosion potential is perhaps caused by high density of dislocation emerged in rolling process.

Fig.2 displays the variation of corrosion potential on peakaged alloy. It reveals that the corrosion potential remained almost unchanged if pH < 9.0～9.5, then, dropped down with pH elevating. Although aluminium oxides are

Table 1 Microhardnesses and Corrosion Parameters in Various Heat Treatment Conditions

Heat Treatmnnt Conditions	Hot rolling	Solution treatment(803 K, 1 h)	Artificial aging (443 K)		
			Underaging (4 h)	Pcakaging (50 h)	Overaging (80 h)
Microhardness(HV)	88	146	161	185	173
E_{corr}(V vs SCE)	−0.72	−0.623	−0.667	−0.731	−0.735
Rp (Ω)	183	280	939	227	234

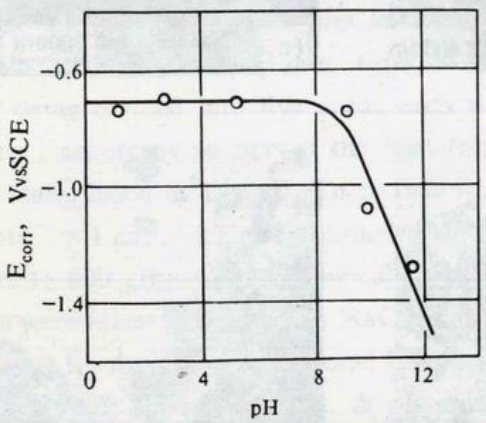

Fig.2 Effect of pH on corrosion potential E_{corr} of the alloy at peakaged state

soluble in both high and low pH solutions[15], the result in Fig.2 indicates the film on this alloy is relatively steady in acidic condition. The reason for corrosion potential dropping in alkaline solution is that the OH^- ion is the most aggressive anion to passive film on aluminium[16]and thus caused a serious corrosion.

4 VARIATION OF CORROSION POTENTIAL IN 24 h IMMERSION DURATION

Fig.3 illustrates the variation of corrosion potentials under various heat treatment states with immersion time in 3.5% NaCl of pH5.4. On peakaged and overaged specimens the corrosion potentials are almost held at constant values, whereas those on other specimens decrease on the whole but fluctuate frequently. Their minimums shift electronegatively towards steady values . Their maxumums first drop and then rise to higher levels . The maximums on hot rolled and underaged specimens recover to near their initial corrosion potentials , however, natural aged alloy is still more than 100 mV negative to its initial value. It can be found that both the speed and extent of corrosion potential dropping are dependent on heat treatment condition. In Rinker's findings it was on underaged state rather than on natural aged state a 2020 alloy appeared that the corroaion potential dropped to negative value. Further work is needed to explain the difference.

After 24 h immersion it is shown the specimens has been corroded to different extents. Concentrated small pittings are uniformly distributed over the surface of hot rolled alloy. On natural aged , peakaged and overaged specimens uniform film and a few pittings developed. The underaged alloy behaves uniquely by developing some film free zones as well as pittings on its surface. Corrosion behavior of the alloy is related to its corrosion potential variation, so it is employed to explain the corrosion potential shifting in Fig.3. On peakaged or overaged specimen, the preferential dissolution of the anodic grain boundary[17,18]can protect most parts of the surface, and, the ratio of anodic area to protected area is very low, so the activation and passivation of a little amount of pitting and a narrow grain bounda-

ry will not disturb the corrosion potential. Since most parts of their surfaces are steady, their corrosion potentials are held unchanged . To the specimens under other states, because their grain boundaries lack precipitates and PEZ, preferential dissolution of the grain boundary does not occur. Their corrosion potentials are controlled by corrosion behavior of matrix. Generally, activation of the material causes corrosion potential dropping , but vice versa in passivation, Therefore, the fluctuation of corrosion potentials reflects the occurrcnce of localized corrosions which accompany potential change. With prolonging immersion time, the solution near electrode / solution interface will vary and shows a higher pH as the result of reaction of lithium with water[19,20]. It is beneficial to repassivation of active area and thus causes maximums of corrosion potenrial to rise. Simultaneously, it can also enlarge the area of active zones to result in the minimums shifting towards steady values at which the dissolution reaction carry on. Therefore, the fluctuating range of corrosion potential is larger in later immersion period. The nonrecovery tendency of the corrosion potential on natural aged alloy implies that this alloy tends to be corroded alomst uniformly at low potential. The preferential dissolution of fine GP zones is probably responsible for its corrosion potential dropping. On underaged alloy, after exposed anodic δ' phase dissolving, relatively cathodic matrix on the surface will suffer slight aggressiveness, assisting the repassivation of active positions. Hence, the maximum of its corrosion potential starts to rise earlier. The film free zones on it probably cause the earlier dropping of its minium. It can be found that a relatively long constant corrosion potential period exists on hot rolled alloy. Lower polarization resistance of it can result in rapid formation of a layer of corroded product which can hinder the transportation of ions, so only uniform corrosion happens and thus the corrosion potential does not change in this period. Nevertheless, with immersion time prolonged, small pittings occurred under the poor protective product, causing the fluctuation of corrosion potential at a later stage on this alloy.

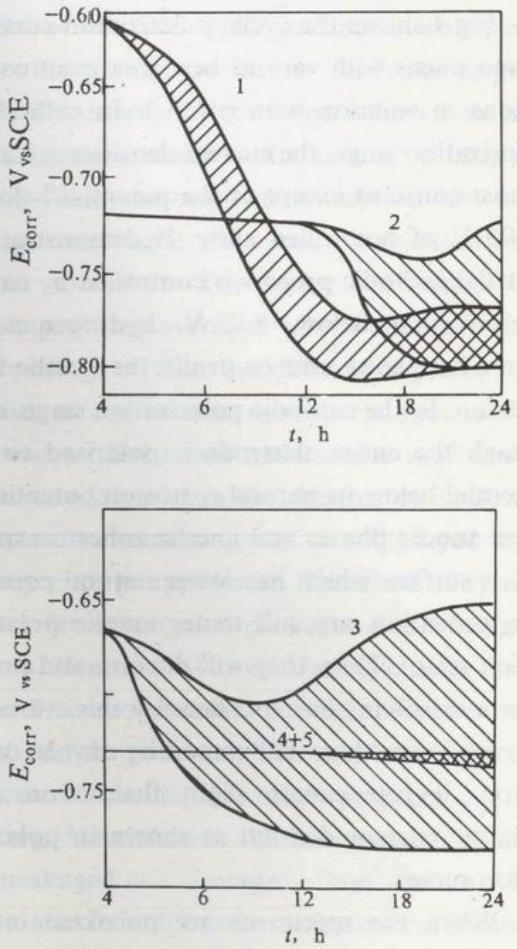

Fig.3 Variation of corrosion potential E_{corr} with immersion time t at the heat treatment state in Table 1

1——natural aged; 2——hot rolled; 3——underaged; 4——overaged; 5——Peakaged

Similar to the results obtained from seawater exposure tests on other alloys[21], the

corrosion behavior mentioned above is not totally the same as that obtained from long period immersion test, in which hot rolled alloy tends to be unifirmly corroded and underaged specimen has the least weight loss. Probably it results from the differences between the property of their corrosion product and between their susceptibility to solution attack.

5 EFFECT OF HEAT TREATMENT ON CYCLIC POLARIZATION CURVE

Fig.4 shows the cyclic polarization curves of specimens with various heat treatment conditions in solution with pH 5.4. In cathodic polarization stage, the current densities remain almost constant except at the potential below −1.05 V of hot rolled alloy. It demonstrates that the cathodic process is controlled by oxygen diffusion. Below −1.05 V , hydrogen evolution happened and controlls the cathodic reaction. In the cathodic polarization stage, although the entire electrode is polarized to a potential below its natural corrosion potential, some anodic phases and anodic zones on specimen surface which has lower natural corrosion potentials are still under anodic polarization state . Thus, they will dissolve and produce a dissolving current. Because this current is much lower than that caused by oxygen diffusion, it just causes slight fluctuation of cathodic current density, as shown in polarization curves.

When the specimens are polarized into anodic stage , only within 10mV polarization the anodic current densities are stimulated to high levels. No passivation tendency emerged on any of the specimens indicates that the alloy at these heat treatment states can not be ptotected by applying anodic polarization in this solution. The curves also revveal that the breakdown potential is equal to or below its corrosion potential. It means all the specimens are susceptible to pitting attack or other localized corrosion. The morphology of a pitting formed in anodic polariza- tion duration, as shown in Fig.5, reveals that under a polarized state the alloy dissolved Preferentially along

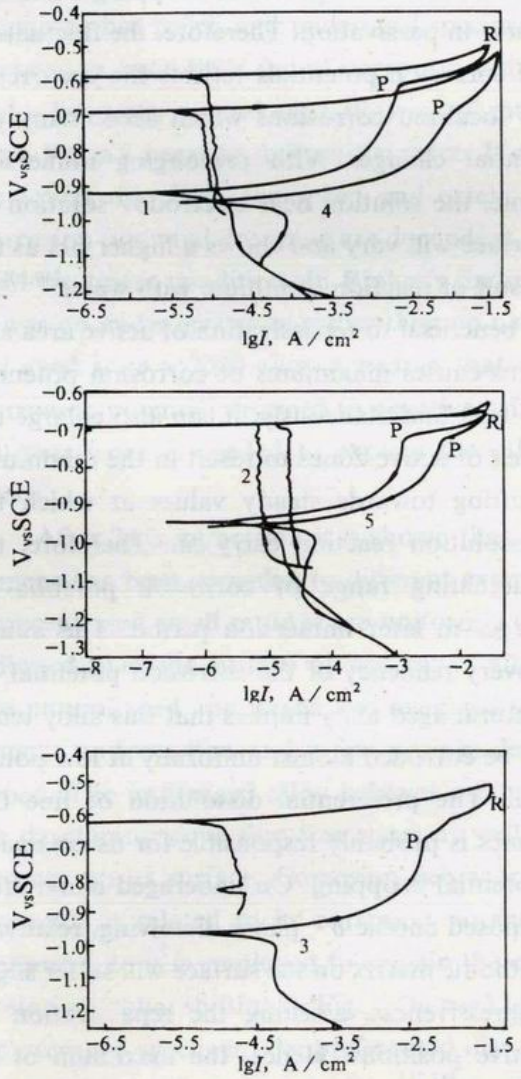

Fig.4 Cyclic polarization Curves of Specimens with various heat treatment in 3.5% (pH5.4) NaCl

1—natural aged; 2—hot nolled; 3—underaged; 4—overaged; 5—peakaged

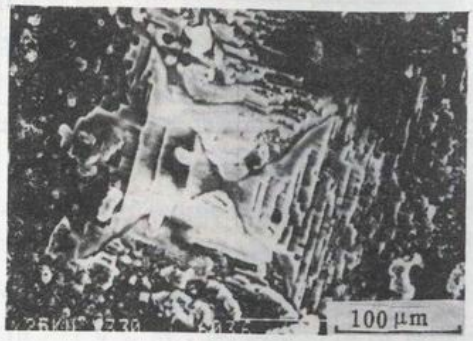

Fig.5 SEM micrograph of a pitting on underaged alloy after anodic polarization in a 3.5% (pH5.4) NaCl

definite crystallographic detections.

After the scan was reversed, polarization current density on each specimen drops down with potential lowering. Every specimen remains anodicly polarized until a new corrosion potential near −0.900V is reached, which is more negative than the initial corrosion potential and near the natural corrosion potential of pure aluminium[22]. In the anodic polariza- tion stage after scan reversing, the curve on each specimen consists of two sections.

It can be assumed that both pittings and uniformly anodic dissolution have occurred on the alloy surface during the anodic polarization period before scan reversing . After scan reversing, the protection process of these two parts occurs in two steps in series. The upper section RP indicates repassivation of pittings. When potential drops to spot P the growth of pittings will totally stop. So the potential at spot P is considered as protection potential of pitting. With further potential dropping from spot P, the still uniformly and anodicly dissolving part will be gradually protected, so the anodic current density decreasses gradually to zero, at which time the potential reaches the new corrosion potential. From the result that the new corrosion potential was close to that of pure aluminium, it is deduced that the preferential dissolution at the earlier stage changes the chemical composition of the alloy on the surface into nearly pure aluminium.

By careful comparison, one can find the form of the upper part of the hysteresis loop representing pitting repassivation is dependent on heat treatment. On hot rolled and natural aged specimens the potential differences between spots R and P are lower than the differences of artificial aged specimens, which implies the pittings on former are easier to protect. This is why the corrosion behavior on hot rolled alloy is easier to change from pitting into uniform corrosion in immersion test and why natural aged alloy tends to manifest uniform corrosion. The larger differences of peakaged and overaged alloys illustrate that the pittings on them are difficult to protect. In addition, the current density changes in RP section on hot rolled and natural aged specimens are larger than the changes on artificial specimens. Immersion test has displayed that heavy pittings appears on hot rolled alloy but just a few pittings on peakaged and overaged alloys. Hence , the current density change from spot R to spot P stands for the amount of pitting, and the potential difference between them represents the repassivation property of the pitting. Nevertheless, the intergranular attack of peakaged and overaged alloys[18] can not be evaluated from the polarization curves because the dissolving current of grain boundary is very low. To underaged alloy, short period immersion test demonstrates it is susceptible to pitting attack, whereas long period immersion test reveals it has high corrosion resistance but still remains the film free zones. The relatively potential difference between spot R and spot P

suggests that it is susceptible to pitting attack. Its RP section also consists of two parts, probably is responsible for its unique corrosion behavior.

When the scan was developed into cathodic stage, the artificial specimens also shows speciality, namely reduction peaks emerge and its height increase with aging time . It has been reported that the peak reflects the reduction of some metal ions from corrosion products on oxygen absorption. Because of no reduction peak emerges on hot rolled and natural aged alloys the reduction peak results from the reduction of dissolved precipitates. Furthermore, considering the peak emerged obviously on peakaged and overaged specimens which mainly contain T1 phase, it is assumed the reduction of corrosion product converted from T1 phase and containing copper results in the reduction peak.

6 EFFECT OF pH ON CYCLIC POLARIZATION CURVE

Fig.6 displays the cyclic polarization curves with various pH values. In solution with pH1.2 polarization sections before and after scan reversing illustrate that the cathodic process is controlled by hydrogen evolution reaction, which causes a much higher current density than oxygen diffusion does . The polarization curves in both anodic stages represent uniform dissolution, it suggests that in strong acidic solution with great aggressiveness, precipitates and matrix dissolve together in high speeds. Therefore, continuing exposure of new grains originally at subsurface layer delays the change of chemical composition near surface into pure aluminium. This is why the new corrosion potential is higher than −0.900 V.

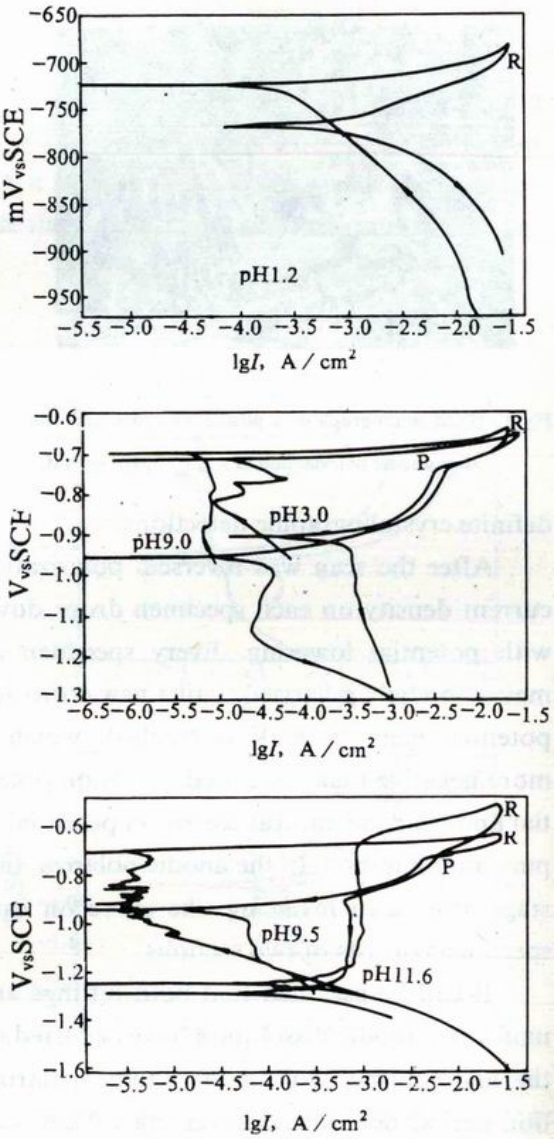

Fig.6 Cyclic Polarization Curves of peakaged alloy in a 3.5% NaCl with various pH values

In weak acidic solution with pH 3.0 the obvious fluctuation of current density in initial cathodic stage reflects the competition between hydrogen evolution and oxygen absorption on the electrode interface. It implies hydrogen evolution is slowed down with pH rising . Its upper part of hysteresis loop reflects that, in solution with pH 5.4, more pittings tends to emerge but they are easier to protect. The

reason for the disappearance of its reduction peak is that the corrosion product is relatively soluble in acidic solution.

When pH was adjusted into weak alkaline the greater fluctuation with larger amplitude of initial cathodic current density and its decrease on the whole reflect that the dissolution of some anodic phases increase in solution containing a large amount of OH^-. In sloution with pH 9.5, at the beginning of polarization the corrosion potential is −1.015 V, but it shifts towards −0.700 V with scanning. According to Fig.2, this shifting reflects the variation of pH at electrode / solution interface towards lower level accompanying the release of H^+ from the cathod. Its small reduction peak indicates that the corrosion product is also soluble in alkaline solution.

The curve in the solution with pH 1.6 shows that the alloy has passivation tendency. But its passivation current density is high and the passivation peak does not appear , implying its passive film is a poor protective. The existence of a turning point in the scan reversed anodic polarization section indicates that in its anodic dissolving stage pittings and uniform dissolution also happened simultaneously. It can be found the breakdown potential in this case is close to the corrosion potentials in solutions with various pH values. Fig.6 shows that the peakaged alloy had essentially the same breakdown potentials and protection potentials. It suggests these potentials are independent of pH change. The curve also reveals that after the potential is reversely scanned to corrosion potential of pure aluminium the current density does not lower further. This illustrates that in alkaline solution uniform dissolution can even happen under the poor protective passive film. The same passivation current densities before and after scan reversing occur because the chemical composition of the film does not change.

7 CONCLUSIONS

(1) Precipitates emerge in the alloy during artificial aging process. In underaged alloy the main intensifying phase is δ'. In peakaged and overaged specimens the amount of δ' decrease accompanying heavy precipitation of T1 phase in matrix and the occurrence of PFZ and precipitates containing high copper along the grain boundary.

(2) Intergranular attack on peakaged and overaged alloys results in their corrosion potentials holding at almost constant values . The development of pittings of other anodic areas causes the fluctuation of corrosion potentials on hot rolled, natural aged and underaged alloys.

(3) The alloy under all heat treatment states is susceptible to pitting attack on solutions ranging from weak acidic to strong alkaline . The prolonging of artificial aging treatment is beneficial to the decrease of pitting but makes them difficult to protect as a result of increasing the difference between the breakdown potenial and the protection potential.

(4) In strong acidic solution the alloy dissolves uniformly but with a corrosion potential the same as those in solutions ranging from weak acidic to weak alkaline. In solutions with higher pH, pittings and uniformly anodic dissolution are occurred together . The increase of solution basicity causes more serious corrosion and lower corrosion potential as well as a poor protective passive film.

(5) With the potential dropping after scan reversing, pittings and uniformly dissolving zones are protected in series. The breakdown

potential and protection potential of the alloy are independent of pH value.

REFERENCES

1 · Niskancn, P., Sanders, T. H. Jr, Rinkcr, J. G., Marek, M.. Corro. Sci. , 1982, 22: 283

2 Moran, J. P., Starke, E. R., Stoner, Jr. G. E., Cahen Jr. G. L.. Corro. , 1987, 43: 374

3 Kumai, C., Kusinski,J., Thomas, G., Dcvinc, T.M.. corro. 1989, 45: 294

4 Chirstodoulou, L., Struble, L., Pickers, J. R.. In: Starkcc, Jr. E. A. *et al* (eds). Aluminium Lithium Alloys. II , AIME, PA, Warrendalc, 1984, 561

5 Ohsaki, S., Takahashi, T. J.. Jpn. Inst. light Met. , 1989, 39: 431

6 Rinker, J. G., Marck, M., Sanders Jr, T. H.. In: Starkcc, E. A. *et al*(eds). Aluminium Lithium Alloys. II AIME. PA, Warrrendalc. 1984, 597

7 FDC long, H., Martens, J. H. M.. Delft Aluminium, 1985, 61: 416

8 Balasubramanian, R., Duquctte, D. J.. Aluminium Lithium Alloys. V, Vol. 3, Birmingham: Matcrials and Component Engincering Pub. Ltd. , 1989, 1271

9 Ricken, R. E., Duquette, D. J.. In: Starkce, Jr. E. A. *et al* (eds). Aluminium Lithium Alloys. II . AIME. Warrendaale. PA, 1984, 581

10 Craig, J. R., Newmen, R. C., Jarrett, M. R., Holroy, N. J. H.. In: Champier, G. *et al* (eds). Aluminium Lithium Alloy. IV. France J. Phys: 1987, 48, C3–825

11 Ohsaka, S., Sato, T., Takahashi, T.. J. Jpn. Inst. Light Met, 1988, 38: 264

12 Sater, J. M., Sanders Jr, T. H.. In: Sanders, T. H. *et al* (eds). Aluminium Lithium Alloys. V, Vol. 3. Birmingam: Matreials and Component Engincering Pub. Ltd. , 1989: 1217

13 Buchheit, R. G., Stoner, G. E.. In: sanders, Jr. T.H. *et al* (eds). aluminium Lithium Alloys. V. Vol. 3, Birmingham: Materials and component Engincering Pub. Ltd. , 1989, 1347

14 Fontana, M. G., Greene, N. D.. Corrosion Engincering. New York: McGraw–Hill Inc. , 1978

15 Pourbaix, M.. Atlas of Electrochemical Equilibrium Diagams in Aqueous Solutions, NACE. Houston Texas: 1974

16 Foley, R. T., Trazaskoma, P. P.. Corro. , 1977, 33: 435

17 Reboul, M., Meyer, M.. In: Champier, G. *et al* (eds). Aluminium Lithium Alloys. IV. France J, phys. , 1987, 48; C3–881

18 Holroyd, N. J. H., Gray, A., Scamans, G. M., Hermann, R.. In: Baker, C. *et al* (eds). Aluminium Lithium Alloys. III The Institute of Metalc, Londom: 1986, 310

19 Srivatsan, T. S., Bobesk, G. E., Sudarshan, T. S., Molian, P. A.. In: Sanders, Jr. T. H. *et al* (eds). Aluminium Lithium Alloys. V, Vol. 3, Birmingham: Materials and Component Engineering Pub.Ltd, 1989, 1237

20 Schumacher, M.. Seawater Corrosion Handbook. New Jersy: Noyes Deta Corp. 1979

21 Groover, R. E., Lennox, T. J., Peterson, Jr. M. U.. Mater. Prot. , November, 1964: 25

22 Drogowska, M., Brossard, L., Menard, H... Corro, 1987, 43; 549